Ultrasonic studies of radiation damage in an aluminum-manganese alloy

D. L. Johnson,* G. G. Setser,† K. L. Hultman,‡ J. Holder,§ and A. V. Granato
Department of Physics and Materials Research Laboratory, University of Illinois at Urbana-Champaign, Urbana, Illinois 61801
(Received 8 January 1985)

A technique has been developed for ultrasonic studies of the properties of crystals containing defects produced by electron radiation of dilute alloys. The method permits measurements of both relaxation and resonance effects for multiple defects for all three independent elastic modes in cubic crystals at low enough defect concentrations to avoid defect interaction effects. A multiple-peak structure was found in an aluminum-manganese alloy. This together with annealing data indicates that more than one defect configuration was present, despite optimum conditions for avoiding complications due to multiple-interstitial and multiple-solute-atom complexes. The major defect is a strongly trapped ⟨100⟩-symmetry mixed dumbbell which rotates between equivalent positions near 130 K at 10 MHz. Existing theories predict some but not all of the effects found. In particular, the fact that the mixed dumbbell rotates between equivalent positions at high and not low temperature, and that this defect configuration does not increase in concentration with annealing, remains as challenges to theory. Also the fact that the multiple peaks found differ greatly from those found in Al-Fe suggests that other aspects besides size effects should be taken into account. The results show that the technique should also be valuable for studies of other alloys.

I. INTRODUCTION

In recent years, several different experimental techniques have been developed to study the interaction of impurities with intrinsic point defects. The most potentially powerful of these seems to be that of ultrasonic measurements at megahertz frequencies as described by Granato,[1] because such measurements should directly yield the symmetry and dynamics of isolated defects. This potential, however, has been largely unrealized for radiation-damage studies because of numerous technical difficulties. We describe a measurement technique which overcomes these difficulties and present the results of the first application to interstitial-impurity interactions in a dilute Al-Mn alloy.

The earliest technique for radiation-damage studies was measurements of resistivity changes, which give information about the dynamics but not of the configurations of interstitial-impurity complexes. Resistivity measurements on pure aluminum and dilute aluminum alloys (~ 0.1 at. %) by Ceresara *et al.*[2] and others[3,4] showed that the addition of foreign atoms could have a pronounced effect upon the thermal recovery of the defects produced by radiation. The characteristic behavior observed in these experiments was a decrease in the recovery in stage I (interstitial recombination with close pair vacancies and long-range migration near 40 K) and an increase in the recovery in stages II and III (vacancy migration near 230 K) when foreign atoms were added to the samples. Damage-rate studies using electrical resistivity measurements on copper alloys by Dworschak *et al.*[5] gave strong evidence that migrating interstitials could be trapped by foreign atoms. More recently, measurements techniques sensitive to the configuration of the defects have been developed and applied. These are channeling, Mössbauer, and internal friction studies.

Channeling measurements by Swanson *et al.*[6] on an irradiated Al-Mn alloy indicated that manganese atoms were displaced by trapped interstitial aluminum atoms up to a temperature of about 180 K, and the pair occupied the ⟨100⟩ tetragonal symmetry "mixed-dumbbell" configuration. Swanson and Maury[7] extended the channeling measurements to other aluminum alloys and found that the trapping configuration was the ⟨100⟩ dumbbell also for alloys of Al-Ag and Al-Zn, but not for Al-Sn. These results are in accord with a simple theory by Dederichs and co-workers[8,9] based on atomic-size misfit considerations. The interpretation of channeling measurements suffers from the fact that (a) relatively high defect concentrations are required and (b) a symmetry determination depends on model calculations which suppose the presence of only one type of defect. In fact, the symmetry found for Al-Fe is in conflict with results found for lower defect concentrations from Mössbauer and internal friction measurements.

Also, Wollenberger[10] and Dworschak *et al.*[11] found that their electrical resistivity damage-rate results were inconsistent with the assumption that the trapped interstitial occupied only one configuration with a single binding energy. They indicated that their results could only be understood by assuming a series of trapping positions having different depths and hence only some of the trapping positions could become unstable at a given temperature. They claimed that the mixed-dumbbell interstitials observed by channeling measurements could only be a small fraction of all the interstitials trapped at temperatures around 50 K. They suggested that other configurations with the interstitial placed at the nearest or next-nearest neighbor of the foreign atom were not observable by the channeling technique.

Rehn *et al.*[12] applied a low-frequency internal friction technique to an Al-Fe alloy and found that there are several defects present simultaneously, none of which could be identified as the expected mixed dumbbell. They stressed the general advantages of internal friction techniques for defect studies. Measurements with the ultrasonic technique described here are complementary to the lower-frequency internal friction measurements and have the additional advantages described by Granato.[1]

II. APPARATUS AND EXPERIMENTAL TECHNIQUES

Al-Mn was chosen as the alloy for this experiment. Manganese has greater solubility in aluminum than iron, and Vogl and co-workers[13–15] supposed that Al-Mn should be similar to Al-Fe. In addition, both resistivity and channeling measurements have been performed on Al-Mn.

The Al-Mn (Mn content nominally 0.1 at.%) sample was prepared from a boule of a $\frac{3}{4}$-in.-diam single crystal. A $\approx$1-cm^3 cube was excised from the boule with an acid saw and then electrochemically polished so that the faces were flat and parallel. A spectrophotometric analysis of two small pieces cut from the boule indicated a concentration of manganese for the front and rear faces of the sample of 0.0974 and 0.081 at.%, respectively. A measurement of the resistivity ratio of a resistivity specimen indicated a concentration of 0.084 at.%.

The ultrasonic vibrations in the sample were generated by unplated, $\frac{1}{2}$-in.-diam, 10-MHz quartz transducers which were bonded to the sample by Nonaq stopcock grease. The sampled-cw technique, recently reviewed by Bolef and Miller,[16] was used for the velocity measurements. In this technique, changes in the resonant frequency f are measured and the corresponding changes in the elastic constant C are calculated from

$$\Delta C/C = -\Delta L/L + 2\Delta f/f \,, \tag{1}$$

where the term $\Delta L/L$ takes into account the change in sample length L.

Ultrasonic measurements of the decrement were performed using a standard pulse-echo technique at frequencies of 10 and 30 MHz. In this technique, the attenuation of two selected echoes is measured and the decrement is then calculated using the standard relation

$$\Delta = \alpha/(8.68f) \,, \tag{2}$$

where α is the attenuation in dB/μsec and f is the frequency in MHz. Plots of the decrement versus temperature were made automatically during the experiment by connecting the analog output of the attenuation unit to a strip-chart recorder and sweeping the temperature with the temperature controller described later. This was found to be particularly convenient when searching for relaxation effects.

To allow for the introduction of defects into the sample at low temperatures, the cryostat design had to provide access to the sample by the electron beam and relatively high cooling power ($\approx$15 W). These requirements were met by modifying the design of a model No. 10DT Dewar purchased from Janis Research Co. (Stoneham, Mass). A sketch of this design, which illustrates the method of cooling, is shown in Fig. 1. The flow of liquid helium from the helium chamber (under 2.5 psi pressure) to the vaporizer is controlled by a throttle valve. Electrical power is supplied to the vaporizer to convert the liquid to cold helium gas before admission to the sample chamber. The throttle valve and vaporizer power are adjusted to provide optimum cooling. It was found that the use of a flowmeter to measure the rate of helium gas exhaust greatly facilitated this operation.

All irradiations were performed with an electron beam from a Van de Graaff machine with energy of about 2.4 MeV and an electron-beam current of approximately 5 μA. The temperature of the sample was maintained at 65 K during the irradiation.

The temperature of the sample was measured with a platinum resistance thermometer and a carbon resistance thermometer. A four-terminal ac bridge was constructed for each thermometer; the bridge for the carbon thermometer was modeled after the ones published by Ekin and Wagner[17] and Zair and Greenfield,[18] while the platinum thermometer bridge was modeled after the bridge published by Kirby.[19] An effort was made to check the bridge thermometry and the reproducibility was found to be approximately 10 mK from 5 to 200 K.

A temperature controller was designed and constructed for this experiment with adjustable proportional band, rate, and reset controls. These controls were adjusted to provide a fast response and very small (<1 mK) steady-state error.

A four-terminal ac bridge was designed and constructed for measuring the resistance of the resistivity sample. The bridge was an unbalanced version of the platinum thermometer bridge of Kirby[19] discussed earlier. The bridge

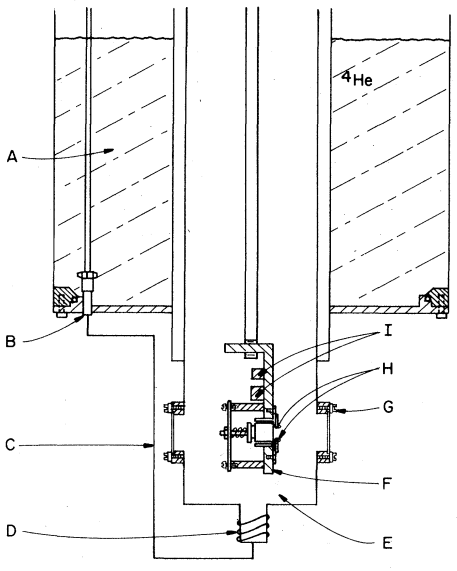

FIG. 1. Cross section of interior cryostat assembly. *A*, helium Dewar; *B*, throttle valve; *C*, capillary tubing; *D*, vaporizer; *E*, sample chamber; *F*, sample holder; *G*, window for electron beam; *H*, resistivity samples; and *I*, carbon and platinum resistance thermometers.

TABLE I. Determination of average concentration in a thick sample of aluminum. (L is the length of the sample.)

Initial electron energy (MeV)	$c_{\text{thin}}/c_{\text{thick}}L$ (cm^{-1})
3.0	2.07±0.06
2.8	2.27±0.05
2.6	2.50±0.06
2.4	2.78±0.07
2.2	3.08±0.08
2.0	3.43±0.12

was found to have a resolution of 10 ppm for resistances of 1 mΩ or higher and an accuracy of 1% or better.

The thickness of the ultrasonic sample ($\sim$1 cm) employed for this experiment was considerably larger than the penetration depth of 2.4 MeV electrons in aluminum ($\sim\frac{1}{2}$ cm). Consequently, the electrons were stopped in the sample and a nonuniform concentration of defects was obtained. Since the diaelastic and paraelastic effects studied in this experiment are linear in the concentration of defects, the nonuniformity of the concentration was taken into account by determining the average concentration of defects in the thick sample. For this purpose a calculation was performed to determine the average concentration of the thick sample in terms of the concentration that would be produced in a thin sample (e.g., a resistivity sample) subjected to the same irradiation. The calculation followed the treatment given by Oen and Holmes[20] for the production of defects by x rays in thick samples. The expression obtained for the average fractional concentration was

$$c_{\text{thick}}=\frac{\phi t}{L}\int_{E_0}^{0}\sigma_d\left[\frac{dE}{dx}\right]^{-1}dE\ , \tag{3}$$

where ϕt is the dose, L is the sample length, σ_d is the displacement cross section, E is the energy of the electrons, and dE/dx is the energy loss per unit distance. This integral was evaluated numerically using the energy-loss tables of Berger and Seltzer[21] and the experimental data given by Wollenberger[22] for the production rate as a function of energy for the displacement cross section. The results of the calculation are presented in Table I. The error estimates were determined by using the upper and lower limits of the production rates experimentally determined.

III. EXPERIMENTAL RESULTS

The decrement measurements were used to search for relaxation effects. Measurements of the decrement from 5 to 200 K were made as a function of polarization, frequency, and annealing temperature. Although relaxation effects can also be studied with elastic-constant measurements, the greater sensitivity to bond effects and the time-consuming nature of such measurements made this undesirable. Consequently, velocity measurements were used primarily to search for diaelastic effects in the three independent elastic constants C_{11}, C', and C_{44} at temperatures below 65 K.

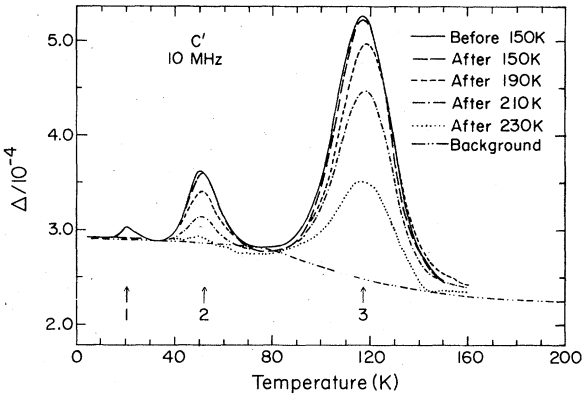

FIG. 2. Measured decrement for the C' mode after irradiation and subsequent annealing treatments. The bottom curve represents the background (or preirradiation) decrement.

The effects observed on the decrement for the C' mode at a frequency of 10 MHz are presented in Fig. 2. The total decrement is plotted in Fig. 2 in order to indicate the size of the effects relative to that of the background (or preirradiation) decrement. Three well-defined peaks (labeled 1, 2, and 3 in the figure) were produced by the radiation and then reduced during the annealing program.

The frequency dependence of the three peaks in the C' decrement is shown in Figs. 3, 4, and 5. In these figures the normalized decrement at frequencies of 10 and 30 MHz are plotted versus the inverse temperature. The normalized decrement Δ_{NT} is defined by

$$\Delta_{\text{NT}}=(T\Delta)/(T\Delta)_m\ ,$$

where the subscript m denotes the maximum value of the product. This procedure was recommended by Nowick

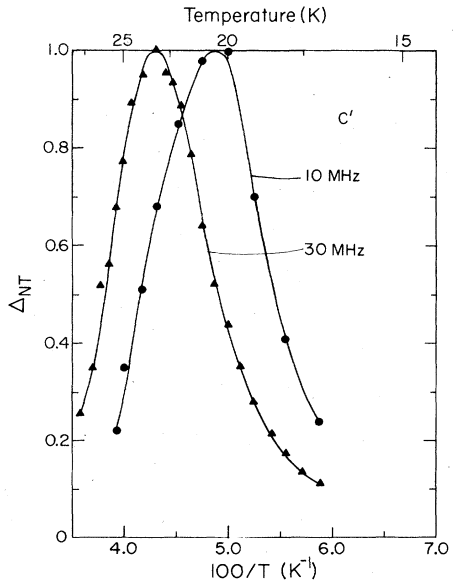

FIG. 3. Frequency dependence of the normalized decrement of peak 1: $\Delta_{\text{NT}}=\Delta T/(\Delta T)_m$.

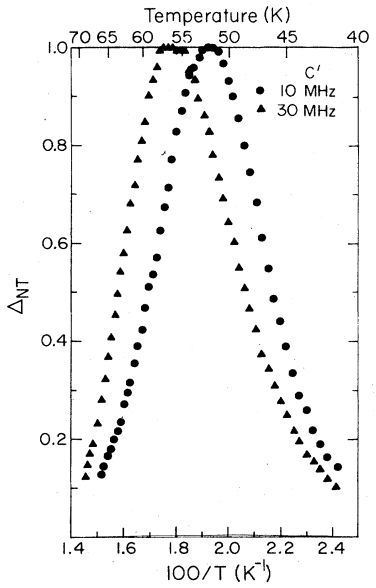

FIG. 4. Frequency dependence of the normalized decrement of peak 2.

and Berry[23] as a method which removes the classical inverse temperature dependence of the relaxation strength and permits an accurate determination of activation enthalpies and frequency factors even when the response is more complicated than a simple Debye behavior. The frequency dependence exhibited by the peaks clearly indicates that the peaks involve thermally activated defect motion.

Measurements for the C_{44} mode decrement were performed at frequencies of 10 and 30 MHz in a manner similar to that employed for the C' mode. However, the results are of much poorer quality, both in accuracy and reproducibility, than those for the C' mode. The reason for this is not completely known. The background attenuation is much higher, with the radiation-produced effects a much smaller fraction of the total attenuation. Also, the reproducibility of the results for the C_{44} mode is about an order of magnitude less than for the C' mode. Also, a peak (or bump) appears in the background near 130 K.

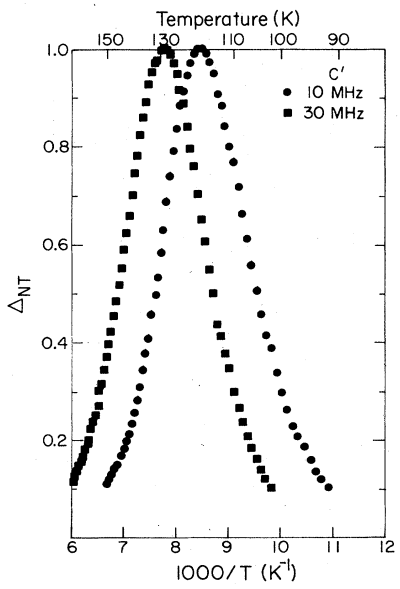

FIG. 5. Frequency dependence of the normalized decrement of peak 3.

The results are shown in Fig. 6 for the decrement as a function of temperature and annealing, with 10-min anneals at 170, 180, 190, 200, and 210 K (the curve for 200 K is not shown). There is a peak at 168 K (peak 4), which anneals during the measurement. The peak has a rather long low-temperature tail. The peak seen at 130 K is not really a radiation-induced peak. It is there before the irradiation and after the annealing. Some annealing occurs in this region (70—140 K), but it appears to be structureless, possibly from the low-temperature tail of peak 4. There is also a small bump near 50 K, but of a size of the order of the sensitivity of the measurement. Several different measurements were made of the decrement for this mode, but the structure found below peak 4 was not well reproduced. The Nonaq bond fails beyond 240 K, preventing a continuation of the annealing program past that temperature.

In summary, for the C_{44} mode there is a peak at 168 K called peak 4, which anneals during the measurement. This corresponds to a defect with trigonal symmetry. The peak at 118 K seems to have tetragonal symmetry. Peak 2 at 52 K is probably tetragonal, but this is uncertain. Peak 1 at 21 K has tetragonal symmetry.

The characteristics of all four peaks are summarized in Table II. The tables lists the temperature at which each peak occurs T_m as well as the frequency factors ν_0 and activation enthalpies H for each peak. To permit a comparison of the different sizes of the peaks, the table also lists the peak height per unit concentration Δ_m/c and the product of the relaxation strength and peak temperature RT_m.

Estimates of the errors for the measured values of the frequency factors and activation enthalpies are also presented in the table. These error estimates were obtained from an error analysis of the frequency dependence of the peaks and are smaller than errors normally obtained from internal friction data. The improved accura-

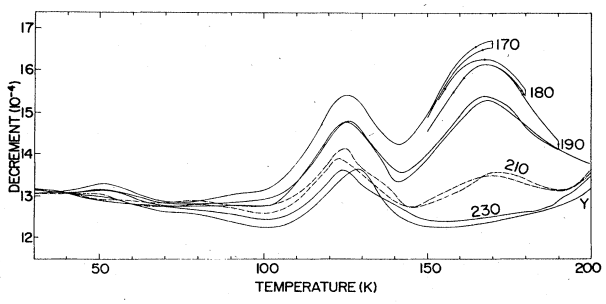

FIG. 6. Decrement at 10 MHz for the C_{44} mode as a function of temperature, for 10-min anneals at 170, 180, 190, 200, and 210 K (200 K not shown).

TABLE II. Measured characteristics of the attenuation peaks in Al-Mn.

Peak number	T_m(10 MHz) (K)	H (meV)	ν_0 (sec^{-1})	Δ_m/c	RT_m (10^3 K)
1	21	20.6±2.5	$10^{12.0}$±0.6	4.0	0.17
2	51.7	73.0±5	$10^{14.1}$±0.5	30	3.10
3	118.5	138 ±2	$10^{12.9}$±0.1	102	24.1
4	168	164 ±10	$10^{11.9}$±0.3	76	25.5

cy is partly due to the fact that a smaller extrapolation to infinite temperature is required on an Arrhenius plot for megahertz frequencies, and partly due to the accuracy of the data.

Measurements were performed of all three independent elastic constants in order to search for diaelastic effects by the irradiation-induced defect pairs. Because of the large temperature dependence of the elastic constants, it was necessary to perform careful measurements of the resonant frequency before irradiation. At low temperatures, a sensitivity of ±1 Hz out of 10 MHz could be achieved. The elastic constant change is related to the frequency change according to Eq. (1). The temperature dependence over the temperature interval of 5 to 30 K of the resonant frequencies for the C' and C_{44} modes in the unirradiated state is shown in Fig. 7. The temperature dependence found for the C' and C_{44} modes did not fit the expected T^4 temperature dependence found for C' and C_{44} in the measurements on pure copper by Rehn *et al.*[24]

The elastic constant changes per unit concentration at 5 K were calculated with the aid of Eq. (1) and are listed in Table III. The small (<5%) length change corrections were computed from the data given by Wagner *et al.*[25] The change in the bulk modulus B listed in the table was obtained from the changes in the elastic constants C_{11} and C', with the aid of data from Kamm and Alers[26] for aluminum.

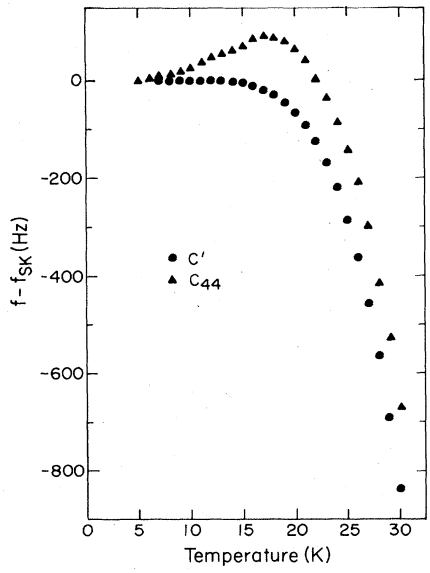

FIG. 7. Temperature dependence of the resonant frequencies for the C' and C_{44} modes before irradiation. $f_{5k}=f(T=5\text{ K})$.

IV. DISCUSSION

It is evident that the multiple-peak structure found here is more complex than was anticipated from the results of the channeling measurements, the interpretation of the Mössbauer-effect measurements, and the mixed-dumbbell model of Dederichs and co-workers. This is despite the fact that the conditions achieved were optimum for the avoidance of complications produced by multiple-interstitial complexes and multiple-solute-atom complexes. We believe that the lack of any indication of complex behavior in the channeling measurements and the Mössbauer-effect measurements is a result of the relative insensitivity of those techniques to multiple and complex defect behavior.

To help identify the predominant relaxation observed in this experiment, the influence of the inverse temperature dependence of the relaxation strength should be taken into account. This was done by multiplying the relaxation strength by the temperature at which the peak occurred, and the results are given in Table II of the preceding section. The corrected values of the relaxation strength show that peaks 3 and 4 are of roughly equal size, with peak 2 being roughly 8 times smaller and peak 1 more than 100 times smaller than either peak 3 or 4. Hence, peaks 3 and 4 are identified as the most prominent peaks in the data.

Additional aid in analyzing the data can be obtained from a comparison of the annealing of the peaks and the resistivity. The effect of annealing on the three peaks is shown in Fig. 8. Since the height of a relaxation peak is

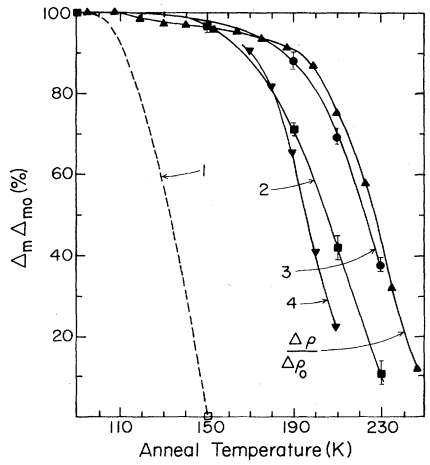

FIG. 8. Comparison of the recovery of the peak heights for peaks 1, 2, 3, and 4 with the recovery of the resistivity [resistivity data from Ceresara *et al.* (Ref. 2)].

TABLE III. Comparison of diaelastic effects with those observed in pure metals and the theory of mixed dumbbells.

	$\frac{\Delta C/C}{c}$			
	C_{44}	C'	C_{11}	B
Pure copper[a]				
all Frenkel pairs	−16	−18	−5	−2
I_D only	−31	−15	−2	0
Pure aluminum[b]	−27	−15		
Al–0.08 at. % Mn (present expt.)	−33.6	−24.7	−20.4	−17.6
Mixed-dumbbell theory[c]	−42.6	−7.5		−6.8

[a]Reference 30.
[b]Reference 28.
[c]Reference 29.

proportional to the concentration of the defect producing the relaxation, the fractional change in the peak heights as a function of anneal temperature is plotted to permit a comparison of the annealing rates. Since each of the peaks anneals at a different rate, it may be concluded that a different defect configuration is responsible for each peak. Figure 8 also contains the resistivity data from Ceresara *et al.*[2] Their data was corrected for the difference in the annealing programs and the difference in concentrations by using the procedure outlined by Nilan and Granato[27] and assuming second-order kinetics. The annealing data in Fig. 8 reveals that peaks 1, 2, and 4 anneal earlier than the resistivity, whereas peak 3 anneals almost simultaneously with the resistivity.

One goal of the present experiment was to test the specific predictions of a model proposed by Dederichs and co-workers[8,9] based on size effects. The model predicts that for undersized impurities, there will exist several trapped positions for an interstitial, with the most predominant one consisting of a caged mixed dumbbell of ⟨100⟩ orientation. In addition, the mixed dumbbell gives a temperature-independent diaelastic reduction of the modulus which is larger for C_{44} than for C'. This model was used to interpret channeling measurements on several alloys and the Mössbauer-effect measurements. The predictions of this model for the present experiment are as follows: (1) The confinement of the defect motion to a "cage" provides an explanation for one deep trap. (A deep trap is defined to be one stable up to stage III.) (2) The symmetry of this ⟨100⟩ mixed dumbbell would produce a peak in the decrement for the C' mode but not for the C_{44} mode. (3) The activation energy for reorientation of the dumbbell within its cage should be less than the free interstitial migration energy of about 120 meV. An analysis of Mössbauer-effect measurements with this model gave a value of the activation enthalpy for reorientation of the mixed dumbbell of 17±5 meV. The behavior of Mn and Fe in Al would be expected to be similar based on size effects alone. A relaxation process with this activation enthalpy would provide a peak in the decrement at a temperature of about 20 K for 10 MHz. In summary, the model predicts a peak near 20 K in the decrement for C' (but not for C_{44}), which anneals in stage III. Other relaxation corresponding to other configurations of the interstitial at weaker trapping positions might occur but in much smaller amounts, and should anneal before stage III. As these anneal, the concentration of the deepest trap configuration (the caged mixed dumbbell) should increase.

No peak was observed in the data which possessed all of the characteristics listed above for the caged mixed dumbbell. For instance, peak 1 occurs in the decrement for the C' mode near 20 K and has an activation enthalpy near 17 meV, but this peak anneals at a temperature much lower than that of stage III. The only peak in C' which is stable up to stage III is peak 3. This peak does have symmetry and annealing characteristics consistent with the channeling data. Also, the fact that peak 3 anneals with the resistivity supports the assumption that it may correspond to the dominant defect. The large relaxation strength of peak 4 corresponding to a defect with trigonal symmetry and its absence in the channeling measurements would then have to be supposed to be due to a trigonal symmetry defect in smaller concentration but with larger dipolar strength. This would make the ultrasonic and channeling measurements compatible by supposing that the major defect is a ⟨100⟩-symmetry mixed dumbbell, but it would not allow the identification of this defect (peak 3) as the caged mixed dumbbell of the model of Dederichs and co-workers because the rotational activation enthalpy (138±2 meV) observed in the ultrasonic measurements is much higher than should be expected from the model.

The diaelastic effect observed in the low elastic constant data was also examined for evidence of mixed dumbbells. Table III presents a comparison of the elastic constant data with data for pure copper by Rehn *et al.*[24] and with data for pure aluminum by Robrock and Schilling.[28] The table also lists the results of the recent theoretical calculation for mixed dumbbells by Zeller and Schober.[29] As can be seen in the table, the elastic constant changes observed here do not have exactly the characteristic pattern expected for dumbbells and hence the diaelastic data does not provide positive evidence for the occurrence only of mixed

dumbbells in this experiment. On the other hand, the measurements give the response from all defects and suggest that there may be a large fraction of the total number of defects which produce a larger contribution to C_{44} than to C'. The diaelastic response to be expected from defects other than dumbbells is not known.

Wollenberger and co-workers[10,11] proposed a multiple-trap model to explain their damage-rate studies using electrical resistivity measurements on several aluminum alloys. This was based on a fit to their measurements, and not on theory. They indicated that their results could not be explained by a model which contained only one major configuration for the trapped interstitial. They listed the following requirements that must be met by a model that would explain their data: (1) The model must have a series of traps of different depths such that only some of the trapping positions become unstable at a given temperature. (2) The model must provide a potential in which the saddle-point energy of the interstitial between trapping positions increases with increasing trap depth for at least some of the directions of approach by the interstitial. (3) There must be at least one trap sufficiently deep so that no final detrapping occurs up to stage III when the foreign atoms are "small."

On the basis of this model, one would expect the following behavior for the decrement measure in this experiment: (1) Immediately following irradiation, peaks corresponding to shallow traps would be observed. (2) During the first part of annealing, the peaks corresponding to shallow traps would disappear and simultaneously the peaks corresponding to deep traps would grow; during the latter part of the annealing (the onset of stage III), the peaks corresponding to deep traps would disappear.

Although some peaks were observed to disappear during the early stages of annealing in this experiment, peak 3 was observed immediately following irradiation and was found not to grow during the annealing before stage III. Hence, this model also does not explain completely the behavior observed here.

The channeling measurements by Swanson *et al.*[6] on an irradiated Al-Mn alloy indicated the presence of $\langle 100 \rangle$ mixed dumbbells which were stable up to a temperature of about 180 K. These channeling measurements are not in disagreement with the mixed-dumbbell model of Dederichs and co-workers as discussed in the preceding section. However, as discussed here, the caged mixed-dumbbell model cannot be used to explain high-temperature relaxation of the mixed dumbbell.

The Mössbauer-effect measurements cited previously were also interpreted with the caged mixed-dumbbell model of Dederichs. Although these experiments were performed with an Al-Fe alloy, Vogl *et al.* pointed out the similarity of the weights and atomic radii of manganese and iron atoms and compared their results with the channeling measurements on Al-Mn. Since the data from the present experiment on Al-Mn are not completely consistent with the model of a mixed dumbbell rotating below stage I, the results of the present experiment are also inconsistent with both the interpretation of the Mössbauer-effect measurements and the assumption that Al-Mn and Al-Fe have similar defect configurations.

Low-frequency internal friction measurements on an Al-Fe alloy were made by Rehn *et al.*[12] No diaelastic effects of the defect pairs were reported, and polycrystalline specimens were used except for one single-crystal measurement giving the C_{44} paraelastic effect. Nevertheless, these authors were able to conclude that the behavior observed in the Al-Fe alloy was inconsistent with the interpretations of the Mössbauer-effect measurements and the recent channeling measurements on an Al-Fe alloy by Swanson *et al.*[31] Since then, Mössbauer measurements[15] on single crystals have provided symmetry information which favors a defect with trigonal symmetry. There remains considerable doubt[32] about the identification of the principal defect complex or complexes for Al-Fe.

The low-frequency internal friction measurements on Al-Fe also revealed a multiple-peak structure which, however, bears little resemblance to that found for Al-Mn in the present experiment. Although the behavior of both alloys was expected to be similar because of the similarity of the weights and atomic radii of the manganese and iron atoms, no clear pattern emerges from a comparison of the data, and the differences are not understood at the present time.

The relative merits for radiation-damage studies of the low-frequency internal friction technique used for the Al-Fe alloy with the megahertz technique developed in the present experiment have already been compared. The technique developed here is also distinguished from the only other application of the megahertz internal friction technique to radiation damage by Rehn *et al.*[24] in the following ways: (1) In the previous study, only elastic constant measurements were used to provide information about the defect behavior. In the present experiment, both attenuation and elastic constant measurements were employed to study the defect behavior and it was shown that the attenuation measurement provided greater speed and reproducibility for measurements over the wide temperature intervals necessary for radiation-damage studies in alloys. (2) Thermal neutron radiation was employed in the studies of Rehn *et al.*, whereas in the present experiment the equipment and specialized techniques necessary for the utilization of electron radiation were developed. The advantages of electron radiation are that it provides less complex damage than neutrons and it is available from the much more accessible Van de Graaff facility. (3) A highly specialized technique that has been developed only for copper was required for the sample preparation in the previous experiment. In the present experiment it was demonstrated that a standard sample preparation technique was sufficient for this alloy and hence the technique offers considerable promise of being easily extended to studies of a wide range of alloys.

Several of the aluminum alloys are promising candidates for future experiments using the ultrasonic technique developed in this experiment. For instance, measurements on an Al-Fe alloy would permit a direct comparison with the low-frequency internal friction results and the Mössbauer results cited earlier for this alloy. In addition, measurements of various other aluminum alloys with different relative sizes of foreign atoms could be used to explore the effect of size differences on the peak struc-

ture and continue the search for evidence for a mixed-dumbbell configuration.

ACKNOWLEDGMENT

This work was supported by the U.S. Department of Energy, Division of Materials Sciences under Contract No. DE-AC02-76ER01198.

*Present address: Const. Engr. Res. Lab, Urbana, IL.
†Present address: Shell Development Co., P.O. Box 41, Houston, TX.
‡Present address: Geomation Corp., Wheat Ridge, CO.
§Present address: CGS, Inc., Austin, TX.

[1]A. V. Granato, *Point Defects and Defect Interactions in Metals,* edited by J. I. Takamura, M. Doyama, and N. Kiritani (University of Tokyo Press, Tokyo, 1982), p. 67.
[2]S. Ceresara, T. Federighi, and F. Pieragostini, Phys. Lett. **6**, 162 (1963).
[3]A. Sosin and L. H. Rachal, Phys. Rev. **13**, 2238 (1963).
[4]M. Doyama, J. S. Koehler, Y. N. Lwin, E. A. Ryan, and D. G. Shaw, Phys. Rev. B **3**, 1069 (1971).
[5]F. Dworschak, H. Schuster, H. Wollenberger, and I. Wurm, Phys. Status Solidi **29**, 75 (1968).
[6]M. L. Swanson, F. Maury, and A. F. Quenneville, Phys. Rev. Lett. **31**, 1957 (1973).
[7]M. L. Swanson and F. Maury, Can. J. Phys. **53**, 1117 (1975).
[8]P. H. Dederichs, Ch. Lehmann, and A. Scholz, Phys. Rev. Lett. **31**, 1130 (1973).
[9]P. H. Dederichs, in *Fundamental Aspects of Radiation Damage in Metals,* edited by M. T. Robinson and F. W. Young (U.S. G.P.O., Washington, D.C., 1975), p. 187.
[10]H. Wollenberger, in *Fundamental Aspects of Radiation Damage in Metals,* edited by M. T. Robinson and F. W. Young (U.S. G.P.O., Washington, D.C., 1975), p. 582.
[11]F. Dworschak, Th. Monsau, and H. Wollenberger, J. Phys. F **6**, 2207 (1976).
[12]L. E. Rehn, K.-H. Robrock, and H. Jacques, J. Phys. F **8**, 1835 (1978).
[13]G. Vogl, W. Mansel, and W. Vogl, J. Phys. F **4**, 2321 (1974).
[14]W. Mansel, G. Vogl, and W. Koch, Phys. Rev. Lett. **31**, 359 (1973).
[15]W. Petry, G. Vogl, and W. Mansel, Phys. Rev. Lett. **45**, 1802 (1980).
[16]D. I. Bolef and J. G. Miller, in *Physical Acoustics,* edited by W. P. Masona and R. N. Thurston (Academic, New York, 1971), Vol. 8, p. 95.
[17]J. W. Ekin and D. K. Wagner, Rev. Sci. Instrum. **41**, 1109 (1970).
[18]E. Zair and A. J. Greenfield, Rev. Sci. Instrum. **44**, 695 (1973).
[19]C. G. M. Kirby, *Temperature: Its Measurement and Control in Science and Industry* (Instrument Society of America, Pittsburgh, 1972), Vol. 4, Part 2, p. 1511.
[20]O. S. Oen and D. K. Holmes, J. Appl. Phys. **30**, 1289 (1958).
[21]M. T. Berger and S. M. Seltzer, *Tables of Energy Losses and Ranges of Electrons and Positrons,* Natl. Bur. Stand. (U.S.) Spec. Publ. No. SP-3012 (U.S. G.P.O., Washington, D.C., 1964).
[22]H. J. Wollenberger, *Vacancies and Interstitials in Metals* (North-Holland, Amsterdam, 1969), p. 215.
[23]A. S. Nowick and B. S. Berry, *Anelastic Relaxations in Crystalline S Solids* (Academic, New York, 1972).
[24]L. E. Rehn, J. Holder, A. V. Granato, R. R. Coltman, and F. W. Young, Jr., Phys. Rev. **10**, 349 (1974).
[25]H. Wagner, F. Dworschak, and W. Schilling, Phys. Rev. B **2**, 3856 (1970).
[26]G. N. Kamm and G. A. Alers, J. Appl. Phys. **35**, 327 (1964).
[27]T. G. Nilan and A. V. Granato, Phys. Rev. **137**, A1233 (1965).
[28]K.-H. Robrock and W. Schilling, J. Phys. F **6**, 303 (1976).
[29]R. Zeller and H. R. Schober, *Proceedings of the International Conference on Lattice Dynamics,* edited by M. Balkanski (Flammarion, Paris, 1977), p. 383.
[30]J. Holder, A. V. Granato, and L. E. Rehn, Phys. Rev. B **10**, 363 (1974).
[31]M. L. Swanson, L. M. Howe, and A. F. Quenneville, in *Properties of Atomic Defects in Metals,* edited by N. L. Peterson and R. W. Siegel (North-Holland, Amsterdam, 1978), p. 372.
[32]K.-H. Robrock and H. R. Schober, J. Phys. (Paris) **65**, 735 (1981).